Available online at www.sciencedirect.com
SCIENCE DIRECT®

Nuclear Science and Techniques, Vol.17, No.6 (2006) 354–369

NUCLEAR SCIENCE AND TECHNIQUES

Basic design of beamline and polarization control

M. WATANABE

(Shanghai Dianji University, Shanghai 200240, China;

Institute of Composite Materials, Shanghai Jiaotong University, China;

Saga University Synchrotron Light Application Center, Japan)

Abstract The basic concept of synchrotron radiation beamlines for vacuum ultraviolet and X-ray experiments has been introduced to beginning users and designers of beamlines. The beamline defined here is composed of a front end, pre-mirrors, and a monochromator with refocusing mirrors, which are connected by beam pipes, providing monochromatic light for the experiments. Firstly, time characteristics of the synchrotron radiation are briefly reviewed. Secondly, the basic technology is introduced as the fundamental knowledge required to both users and designers. The topics are photoabsorption by air and solids, front ends and beam pipes, mirrors, monochromators, and filters. Thirdly, the design consideration is described mainly for the designers. The topics are design principle, principle of ray tracing, optical machinery and control, and vacuum. Fourthly, polarization control is considered. The topics are polarizers, polarization diagnosis of beamline, and circularly-polarized light generation. Finally, a brief summary is given introducing some references for further knowledge of the users and the designers.

Keywords Synchrotron radiation, Beamline, Vacuum ultraviolet, X-ray, Polarization

CLC numbers TH744.15, O435.2

1 Introduction

Synchrotron radiation emitted from high energy electrons moving on circular or undulating orbit is the superior light ranging from infrared to X-ray through vacuum ultraviolet (VUV), having excellent linear and circular polarization characters[1-3]. (The VUV of short wavelength is often called soft X-ray (SX). However, only the term VUV is mainly used in this article). The machines in which high-energy electrons circulate are storage rings, equipped with beamlines for experiments, such as spectroscopy, diffractometry, imaging, and others. The beamline defined here is composed of a front end, pre-mirrors, and a monochromator with refocusing mirrors, which is connected by beam pipes, which serves as the monochromatic light to experimentalists. The beamlines have to be designed and constructed to utilize fully the advantageous characteristics of synchrotron radiation. In this article, the design principle and the performance of beamlines, and the polarization control for VUV/X-ray experiments have been introduced to beginner users and designers of beamlines. Firstly, the characteristics of synchrotron radiation are briefly reviewed. Secondly, the fundamental optical technology achieved so far is introduced, because users have to be well versed in them, and designers of beamlines as well. Thirdly, the design consideration required for constructing beamlines is described. Fourthly, the polarization control is considered. It should be noted that the polarization characteristics of synchrotron radiation are not necessarily transferred to sample positions because of the polarizing action of optical elements. Finally, this article is briefly summarized. Before proceeding to the main subject, a brief review on synchrotron radiation is given below.

The schematic of the storage ring is shown in Fig.

Email: watanabemakoto@163.com

1. Electron beams circulate in a magnet system and are focused by it, though only four bending magnets and an undulator are shown in the figure. The electron beam has the size and the divergence because of small transverse motions of electrons around the central orbit. They are represented by using standard deviations. Recently bright sources with small beam size and divergence called the third generation light source have been developed[3, 4]. In these, the sizes are mm and $\sigma_y = 0.01-0.05$ mm, and the divergences are $\sigma_x' = 0.01-0.05$ mrad and $\sigma_y' = 0.005-0.01$ mrad. These quantities are different at any positions on the orbit. On the other hand, an emittance that is approximately equal to a product $\sigma_x = 0.05-0.5$ t of the size and the divergence is constant at every position. In the third generation light source, the emittance is less than 10 nm・rad in the horizontal plane, whereas less than 1 nm・rad in the vertical plane. The radiofrequency (RF) cavity supplies the energy to the electrons, by an amount of power loss by emitting synchrotron radiation, $P(\mathrm{kW}) = 88.5E^4(\mathrm{GeV})I(\mathrm{A})/\ R(\mathrm{m})$, where E, I, and R are the electron energy, stored current, and radius of the bending magnet, respectively. By this process, the electron beams are bunched and have a pulsed structure, which can be utilized for time-resolved experiments. Electrons circulate under ultrahigh vacuum condition guaranteeing a long lifetime, but vacuum chambers of the electron path are not drawn in the figure.

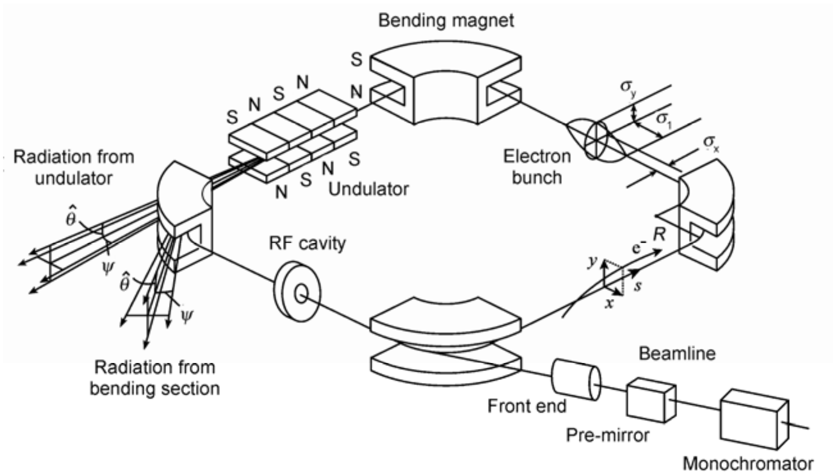

Fig. 1 Schematic of light source and beamline.

The characteristics of synchrotron radiation are as follows[1 - 4]. The radiation from a bending magnet is a smooth continuum spectrum with a maximum near a critical photon energy $u_c(\mathrm{keV}) = 2.22E^3(\mathrm{GeV})/R(\mathrm{m})$. Its vertical divergence is small in high photon energy range, whereas large in low photon energy range. The divergence around the critical photon energy is $\sim 1/\gamma$, where $\gamma = \ 1957E(\mathrm{GeV})$, and much smaller than 1 mrad. It is linearly polarized light on the median plane and elliptically polarized light above and below the plane, practically used as circularly polarized light. The radiation from the undulators is the intense quasi-monochromatic light composed of fundamental and higher harmonics. In many cases, undulators are made of permanent magnets. The photon energy can be chosen by changing the magnetic field of the undulators with changing their gaps. When the gap is changed simultaneously with scanning a monochromator, the peak intensity of the fundamental or higher harmonic light can be used at every photon-energy. It is called synchronous tuning. The divergence of the radiation from an undulator is $\sim 1/\gamma\sqrt{mN_{\mathrm{u}}}$ for both vertical and horizontal directions, where m and N_{u} are the order of harmonic and period numbers of the undulator, respectively. The divergence is of 0.01-1 mrad order. When the magnetic field of an undulator becomes large, the radiation becomes similar to that from bending magnets with an intensity of N_{u} times. It is called multipole wiggler. From planar and helical undulators, linearly and circularly polarized light is obtained, respectively.

The total divergence of synchrotron radiation consists of a divergence of the electron beam and that of the radiation itself. The intensity of the radiation is expressed as a photon number per unit angle/angles of divergence and area. Usually the following three units using the angular coordinate defined in Fig.1 are used.

Flux = photons/s/0.1%bw
(integrated over ψ and $\hat{\theta}$),

Angular flux = photons /s/mrad/0.1%bw
(divided by ψ, integrated over $\hat{\theta}$),

Brilliance = photons /s/mrad^2/mm^2/0.1%bw
(divided by ψ and $\hat{\theta}$),

where mm^2 means cross sectional area of electron beam and 0.1%bw, the fractional band width $\Delta\lambda/\lambda$ of 10^{-3}, where λ is the wavelength. These units are normalized not by mA, but by an operating current.

In the case of radiation from bending magnets the angular flux is useful. The flux is given by a product of the angular flux and an angle of acceptance $\Delta\psi$. The brilliance (often called brightness) is useful for both radiation from undulators and bending magnets. In the case of the radiation from undulators, the flux is given by a product of the brilliance and both horizontal and vertical angles of divergence and beam size. Programs to calculate the intensity are available[5].

2 Basic optical technology

2.1 Photoabsorption by air and solids

The VUV and X-ray are absorbed when they enter the materials. It is because of the excitation of valence electrons and core electrons. When incident light of intensity I_0 enters a matter of thickness d and passes through it, the intensity of transmitted light I becomes $I = I_0 \exp(-\mu d)$, where μ is the absorption coefficient.

In air, the absorption is negligibly small for visible light. Therefore, it can pass through the air. However, for the light, of which wavelength is shorter than about 200 nm, the air becomes opaque because the absorption by O_2 rises. Around 100 nm, $\mu = 8\times10^3\ \mathrm{cm}^{-1}$ in air, so that 90% of the light is absorbed, when it proceeds by only 2.3 μm. Around K edge of N_2 (~ 3.2 nm), $\mu \approx 10\,\mathrm{cm}^{-1}$, and around 1.0 nm, $\mu \approx 1\,\mathrm{cm}^{-1}$ [6], hence the light around these wavelengths can pass the air ranges, but the path length is of the μm order. Therefore the optical path should be evacuated for the usual experiment in the wavelength region between about 200 nm and 0.3 nm and this is the reason why the light is called vacuum ultraviolet. On the other hand, the absorption coefficient for the Cu K_α line (0.154 nm, 8.05 keV) becomes $2\times10^{-2}\ \mathrm{cm}^{-1}$, allowing the light to pass unless the path is long. As the photon energy becomes larger in the X-ray region, the path length becomes larger.

Solids have about 10^3 times larger absorption coefficients than gases. The coefficients are $10^4 - 10^6\ \mathrm{cm}^{-1}$ in the VUV region and $1 - 10^3\ \mathrm{cm}^{-1}$ in the usual X-ray region. Therefore thick optical elements cannot be used in the transmission mode, but only thin elements. They are films/foils for windows and filters, thin crystals for polarizers and dispersive elements, and special focusing lenses with concave shape. Exceptional ones are transmission gratings and zone plates, and prisms, lenses and polarizers made of ionic crystals for the use in VUV region above their cutoff wavelength (shortest cutoff : 105 nm for LiF). They are all used for special purposes and cannot be used generally. Therefore in VUV and X-ray beamlines reflection optics are widely employed rather than transmission optics.

2.2 Front ends and beam pipes

The beamline is connected to the storage ring through a front end. An example of front ends for X-rays is shown in Fig. 2[7]. It consists of a water cooled mask, gate valves, optical and γ-ray shutters, an aperture (collimator), a monitor, a heat absorber made of carbon film, and a Be window. The Be window which bears against 1 atmospheric pressure separates the ultrahigh vacuum of the storage ring from the usual vacuum of X-ray beamline. In the case of VUV beamlines such windows cannot be used, hence the vacuum of beamlines has to be also ultrahigh vacuum. Beam pipes connect the front end, pre-mirror chambers, a monochromator equipped with refocusing mirrors, and pumping stations. Monitors and apertures are situated appropriately between the front end and the monochromator. Even for hard X-rays (HX), long beamlines have to be evacuated or filled by He gas to suppress not only absorption and scattering by air, but also reaction or erosion of beam pipes and other devices with generated active ions. Usually security systems are provided against the deterioration of vacuum.

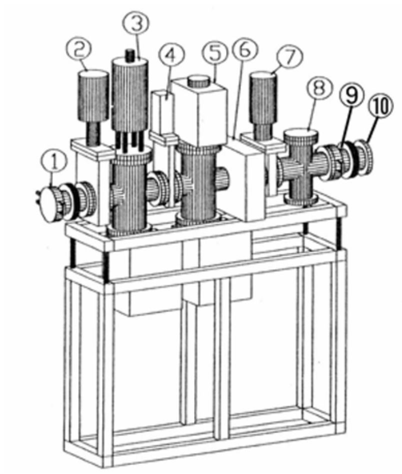

Fig. 2 Example of front end of beamline for X-ray. 1. Water-cooled mask, 2. Metal gate valve, 3. Light shutter, 4. Gate valve using Viton gasket, 5. γ -ray shutter, 6. Aperture (collimator), 7. High speed valve, 8. Monitor, 9. Carbon-film heat-absorber, 10. Be window[7].

2.3 Mirrors

In photon energy below 20 keV, mirrors are often used to gather synchrotron radiation and to focus the dispersed light onto the sample, suppressing the higher order light. Important items are their reflectance and focusing condition.

2.3.1 Reflectance

Here the complex refraction index is defined as $\tilde{n} = n + \mathrm{i}\kappa$ where n is the refraction index, $\kappa = \lambda\mu/4\pi$, the extinction coefficient, and λ, the wavelength. The values of n and κ are available for many materials[8]. In visible region, n is small, whereas κ is large in metals, so that they have high normal-incidence reflectivities as calculated from Fresnel equation and are used in reflection coatings. On the other hand, in VUV and X-ray regions, n is usually a little smaller than 1 and κ becomes smaller with decrease in wavelength for all materials. For instance in fresh Al, $n = 0.044$, $\kappa = 1.18$, and $R = 93\%$ for normal incidence at 10 eV, but at 50 eV, $n = 0.97$ and $\kappa = 0.006$, and $R = 0.03\%$. Therefore in the wavelength region below 40 nm or 30 nm, the grazing incidence optics is employed. In the grazing incidence, the reflectivity increases with the increase in angle of incidence. Furthermore, the total reflection can be utilized, because $n < 1$. As seen in Fig.3, the reflectivity of Au increases with the increase in angle of incidence θ when photon energy is fixed. When θ is fixed, the reflectivity decreases suddenly around the photon energy where the condition of the total reflection is not satisfied, with increase in photon energy. By the use of this feature, mirrors can be used as the reflection filter to reject dispersed light of higher order. The photon energy of the sudden decrease in reflectivity shifts to high photon energy side with increase in angle of incidence. By the use of this feature, one can choose cutoff energy. The grazing angle $\hat{\theta} = 90° - \theta$ is often used in short wavelength region. The critical grazing angle is approximately given as $\hat{\theta}_c \approx \sqrt{2(1-n)} \approx 2.3\times10^{-2}\lambda\sqrt{\rho Z/A}$, where ρ , Z, and A are density ($\mathrm{g\cdot cm^{-3}}$), atomic number, and atomic weight of the coating material, respectively. Unit of $\hat{\theta}_c$ is rad and that of λ is nm.

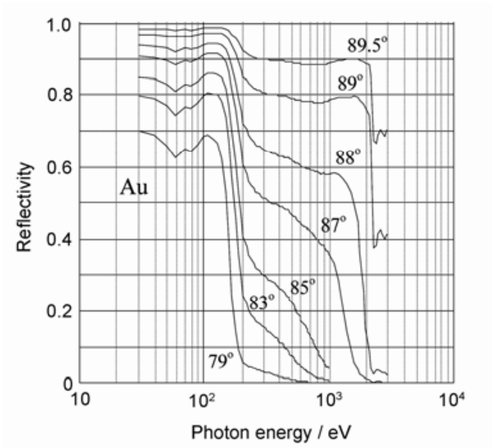

Fig. 3 Reflectivity spectra of Au.

To get high reflectivity especially for high energy X-rays, the mirrors have to be used in extreme grazing incidence. However by the use of multilayers recently developed[9], the situation is somewhat relaxed. The multilayers are composed of two kinds of materials piled periodically. The strengthening interference among the reflected light at the interfaces occurs when condition $2d\sin\hat{\theta} = m\lambda$ is satisfied, where d, $\hat{\theta}$, m, and λ are period length, grazing angle of incidence, order of diffraction, and wavelength, respectively. The reflectivity is enhanced at a certain wavelength λ.

The incident angle $\hat{\theta}$ can be chosen larger than the critical angle of total reflection $\hat{\theta}_c$ for the light of the same photon energy, so that one can use smaller mirrors. When a wide region of high-reflectance is required, a multilayer called supermirror, of which period length changes gradually in depth direction, can be used. The above-mentioned features can be seen in Fig.4[10]. The high reflectivity range of a W monolayer is below 10 keV, that of a W/Si multilayer, around 19 keV and that of a W/Si supermirror, between 18 keV and 22 keV.

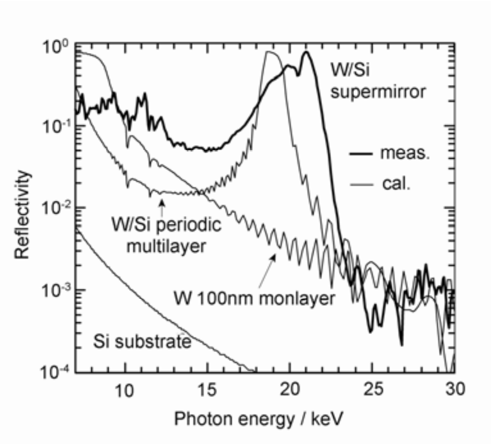

Fig. 4 Reflectivity spectra of W/Si supermirror, W/Si periodic multilayer, W monolayer and Si substrate[10]. Angle of incidence is 0.5.

2.3.2 Focusing

Focusing mirror systems are illustrated in Fig.5[7]. To gather the light, spherical mirrors are widely used, because of relative easiness of fabrication in comparison with aspherical mirrors. When angle of incidence is θ, conditions of tangential and sagittal focusing are given as

$$\frac{1}{r}+\frac{1}{r'}=\frac{2}{R\cos\theta} \tag{1}$$

and

$$\frac{1}{r}+\frac{1}{r'}=\frac{2\cos\theta}{R} \tag{2}$$

respectively, where r, r', and R are the distance from the source to the mirror, the distance from the mirror to the focusing point, and the radius of the spherical mirror, respectively. In exact normal incidence ($\theta=0$), both focusing points coincide, but in grazing incidence they separate and it causes astigmatism. When a point focusing using only one mirror is required, a toroidal mirror, of which tangential and sagittal radii are different, is used. The point focusing using two mirrors called Kirkpatrick-Baez objective, of which reflection surfaces are perpendicular to each other, is widely used.

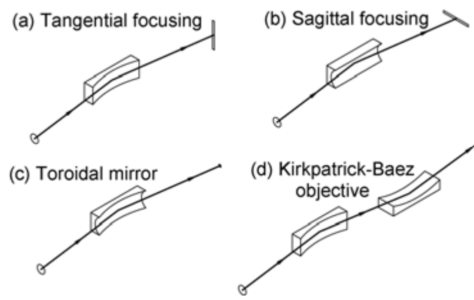

Fig. 5 Focusing mirror systems.

2.4 Monochromators

Nowadays, many kinds of monochromators for the use of synchrotron radiation have been developed under the limitation that the light source can not be moved and the dispersed light is required to come always to the sample position. Dispersive elements are gratings and crystals in VUV and X-ray regions. The schematic diagrams of monochomators are shown in Fig.6. Synchrotron radiation is dispersed by gratings in the wavelength region above 0.5 nm, whereas by crystals below 1.5 nm in usual. The dispersion efficiency is less than 10% for gratings, whereas 80%-90% for crystals (the efficiency is of 10% order around 1 nm because of strong absorption).

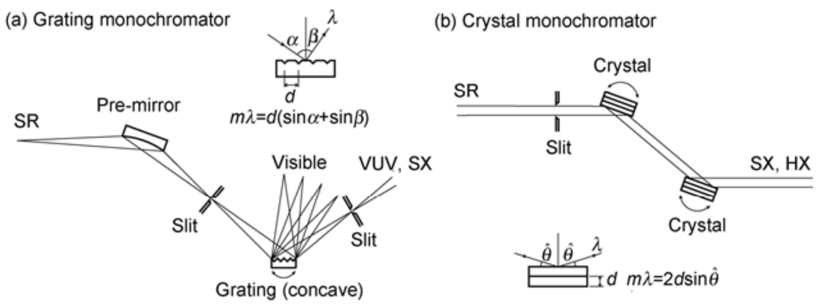

Fig. 6 Schematics of monochromators.

2.4.1 Grating monochromators

The dispersion condition of a plane grating for the parallel incident light is given as $d(\sin\alpha + \sin\beta) = m\lambda$, m=0, ± 1, ±2, ……,where d is a groove space, and α and β are angles of incidence and diffraction, respectively. The band width of the dispersed light is given as $\Delta\lambda = wd\cos\beta \times 10^3 / r'm\,(\mathrm{nm})$, where r' and w are the distance from a focusing mirror to the image formed by it on a slit given in m and the slit width given in mm, respectively. d is given in mm. The resolving power is given by $\mathcal{R} = \lambda/\Delta\lambda = mN$, where N is the number of grooves irradiated by the incident light. However, this equation gives the theoretical maximum and is only valid for ideal cases. It is possible to let even plane grating possess focusing force by varying the groove space gradually one by one in an appropriate way. This is based on the fact that different groove spaces give different diffraction angles, so that even though parallel light irradiates the plane grating, the diffracted light is no more parallel light.

The dispersion condition of spherical gratings is the same as that of plane gratings. The band width $\Delta\lambda$ is also given by the same equation when the aberration effect is neglected. For the spherical grating, the resolving power $\mathcal{R}$ is limited by the optimum width W_{opt} of the irradiated grating area. The tangential and sagittal focusing conditions of a spherical grating of a radius R are

$$\frac{\cos^2\alpha}{r} + \frac{\cos^2\beta}{r'} = \frac{\cos\alpha + \cos\beta}{R} \tag{3}$$

and

$$\frac{1}{r} + \frac{1}{r'} = \frac{\cos\alpha + \cos\beta}{R} \tag{4}$$

respectively. One of the tangential solutions is Rowland solution, where $r = R\cos\alpha$ and $r' = R\cos\beta$. The source and the image points are on the well-known Rowland circle, of which diameter is the radius of the grating. This solution has small aberration. All other solutions are called off-Rowland solutions. In the case of m=0, that is mirror reflection ($\alpha = -\beta$), Eqs. (3) and (4) become Eqs. (1) and (2), respectively. The tangential and sagittal focusing points are different in general. The situation where the source is on a Rowland circle is shown in Fig.7.

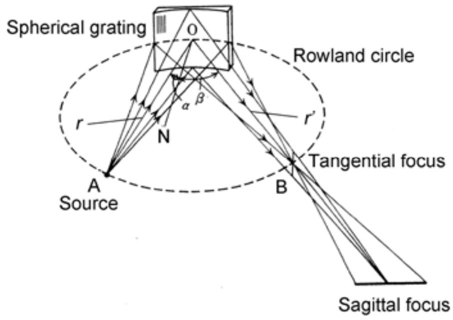

Fig.7 Focus of spherical grating in case that source is on Rowland circle.

In the case of spherical grating monochromators (SGM), on-Rowland mounts have an advantage of small aberration, but their scanning mechanism is very complicated. Therefore, off-Rowland monochromators with simple mechanism, such that slits are fixed or their required movements are small, and gratings are only rotated around a fixed axis, are widely used. They are called constant- deviation type, as $2k = \alpha - \beta$ is constant. In every off-Rowland monochromator, the Rowland condition is satisfied at one wavelength. Such off-Rowland monochromators are of off-plane Eagle, Seya-Namioka, and other types in normal incidence, and of Dragon type shown in Fig. 8 (a)[10], constant-arm type shown in Fig.8 (b)[11, 12], and other types in grazing incidence. Even off-Rowland monochromators can realize high resolution, when gratings of large R are employed. Dragon monochromator is such a monochromator. Its entrance slit is fixed and the grating only rotates, and the exit slit moves a little to ensure good focusing. The original Dragon had a grating of a large radius (57.3 m) and was used in the 4.5-1.5 nm region. $\lambda/\Delta\lambda$ was around 10^4 around 3 nm. The constant-arm one is a little compact, but a combination of the grating and the plane mirror has to be slid along the direction of incident light [13].

Another type of the monochromator widely used is a plane grating monochromator (PGM). In the region from near infrared to ultraviolet, a normal incidence monochromator of Czerny-Turner type is available. It consists of an entrance slit, a collimating mirror, a plane grating, a focusing mirror, and an exit slit. For the use of synchrotron radiation, the PGM is used not only in normal incidence, but also in grazing incidence. Sometimes, the electron beam itself is regarded as an entrance slit. A few or several gratings with different groove densities can be interchanged *in situ*. Old generation PGMs provided several mirrors before or after the grating at different positions for selection of angle of incidence. This has advantages to use the grating efficiently and suppress the higher order light. A developed PGM is of SX-700 type having an ellipsoidal mirror as the focusing mirror shown in Fig.8 (c)[14]. The characteristic of the ellipsoidal mirror that light emitted at one focal point of ellipsoid is focused by the mirror on the other focal point is utilized. A plane mirror moves along the axis of synchrotron radiation, where the angle of incidence always satisfies the condition that the virtual image of the electron beam is at one of the focal points of the ellipsoid. Recently new types of PGMs with varied groove-space gratings have been developed[15-17]. Fig.8 (d) shows an example of such PGMs. The merit of the varied space grating is that the dispersing surface is smooth with small shape error, one can omit one focusing element, and the aberration can be minimized by choosing the most appropriate groove space.

An example of throughput spectra from a PGM equipped with varied space gratings is shown in Fig.9[18]. The radiation from an undulator of "figure 8" type was used. In this case, the integer order light gives the linearly polarized light in horizontal plane ($E_{//}$) and the half-integer order in vertical plane ($E_{\perp}$). Photon number obtained at the sample position is $1\times10^{11}\cdot\text{s}^{-1}$ with $\Delta E/E = 2\times10^{-4}$ at 2 keV at 100 mA of stored current with synchronous tuning. The beam size of $50\,\mu\text{m}$ (w)$\times 10\,\mu\text{m}$(h) is obtained with a mirror system composed of two pre-mirrors and a refocusing mirror.

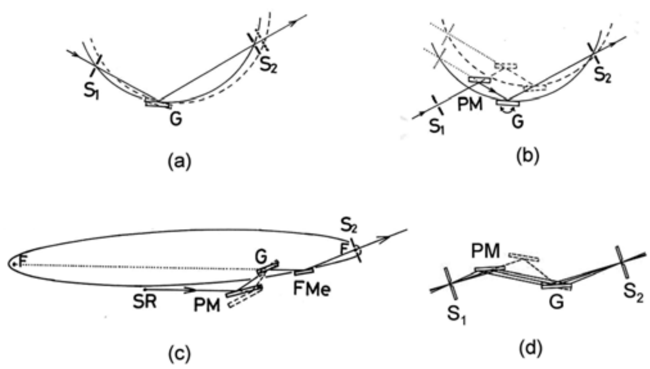

Fig.8 Schematics of grazing incidence monochromators with spherical gratings (SGM) and plane gratings (PGM). (a) Dragon (SGM), (b) Constant-arm (SGM), (c) SX-700 (PGM) and (d) PGM with varied space grating. S_1: Entrance slit, S_2: Exit slit, G: Grating, PM: Plane mirror, FMe: Ellipsoidal focusing mirror.

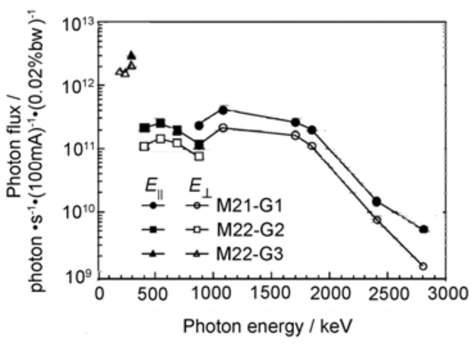

Fig. 9 Throughput spectrum of a plane grating monochromator with varied space grating (SPring-8)[18]. $E_{//}$ represents the signal for the 1st order light from "figure 8" type undulator and $E_{\perp}$, that for the 0.5th order.

2.4.2 Crystal monochromators

In many cases, the monochromatization with crystals is made by reflection mode (Bragg case) and the dispersion condition is given as $m\lambda = 2d\sin\hat{\theta}$, where d is lattice distance. Typical crystals are listed in Table 1 with the useful range when the incident grazing angle can be scanned from 5° to 70°. The crystals are chosen according to the energy region of interest and requirement of resolution. From the dispersion condition, the fractional band width is given as $\Delta E/E = \Delta\hat{\theta}\cot\hat{\theta}$, where E and ΔE stand for the photon energy of monochromatized light and its band width, respectively. $\Delta\hat{\theta} = \sqrt{(\Delta\omega)^2 + (\Delta\tau)^2}$, where $\Delta\omega$ is the inherent divergence of the diffracted beam for the case that the perfect parallel beam enters, and

$\Delta\tau$ is the photon beam divergence. When $\Delta\tau = 0$, $\Delta E/E$ becomes independent of the photon energy. The theoretical fractional band widths are, for instance, 3.2×10^{-4} for Ge (111), 1.33×10^{-4} for Si (111), and 2.3×10^{-5} for Si (400). In the real case, $\Delta\tau \neq 0$. When $\hat{\theta}$ is near $90°$ (backward scattering), $\Delta E/E$ becomes very small. Recently, $\Delta E/E = 10^{-8}$ is achieved, that is $\Delta E = 120$ μeV at E=14.4 keV[19].

Fig. 10 shows schematics of double and 4-crystal monochromators. The most popular crystal monochromators are the double crystal monochromator (DXM). Two crystals are set parallel to each other and rotated for wavelength scanning. Let the incident light shine on the center of the surface of the first crystal, and two crystals rotate as a whole around the center. In the case that the distance between two crystals is fixed, the height of the light dispersed by the second crystal changes with the rotation. Therefore to make the direction and height of the dispersed light fixed, several types of DXMs have been designed and fabricated. In the case of Figs.10 (a) and (b), the rotational axis is located at the surface of the first crystal and the position of the second crystal is adjusted (a) by a computer, and (b) by a mechanical cam[20, 21]. In the case of Fig.10 (c), the L-shaped bar rotates around the axis at its corner. Two crystals are set on the respective sides of the L-shaped bar and slide along the sides[22]. The surfaces of the first and the second crystals are set parallel to the side at which the first crystal is situated. On the other hand, the first crystal is also constrained to move along the incident beam axis and the second crystal along the dispersed light axis. In DXMs, the detuning method is often employed. It utilizes the fact that the angle width of the higher order light is much smaller than that of the 1st order light. Therefore when the second crystal is set at the angle a little apart from the Bragg angle, the purity of dispersed light increases, though decrease in intensity is inevitable. The second crystal is often bent sagitally to focus the dispersed light onto the sample. The focusing conditions are the same as those of mirrors. In DXMs, two crystals are set parallel, so that the resolution is the same as that of the single crystal case.

Fig.10 (d) shows the schematic of a 4-crystal monochromator. The first and the second crystals are set parallel, and the third and the fourth crystals are set parallel. However, the couple of the first and the second crystals are antiparallel to the couple of the third and the fourth crystals, so that high resolution is achieved. Usually, each couple is monolithic, which means that a reflection channel of two facing parallel planes is a part of a single crystal cut out from it. Therefore the parallelism of the two lattice planes is automatically satisfied.

In some cases, the monochromatization is made by the transmission mode (Laue case). The dispersion condition is the same as that of the reflection mode. Recently a transmission type monochromator of Cauchois type has been developed for the use of synchrotron radiation. In this case, thin crystal is bent not only sagittally, but also anticlastically to get high resolution and small beam size[23].

Table 1 Dispersive crystals for X-ray

Crystal	$2d$ / nm	Energy range / keV (Grazing angle 5°-70°)
β-Al_2O_3 (002)	2.253	0.586-6.31
Beryl (1010)	1.5965	0.827-8.91
YB_{66} (400)	1.176	1.12-12.1
$KTiOPO_4$(KTP)(011)	1.095	1.21-13.0
SiO_2 (1010)	0.8512	1.53-16.7
InSb (111)	0.74806	1.72-19.0
Graphite (002)	0.6708	1.94-21.2
Ge (111)	0.6532	1.99-21.7
Si (111)	0.6271	2.07-22.6
Si (220)	0.3840	3.39-37.0
Si (311)	0.3274	4.03-43.5
Si (400)	0.2715	4.86-52.4
Si (511)	0.2090	6.31-68.1

Sometimes asymmetric reflection is used to expand or contract beam widths. In this case, the crystal surface is not parallel to the reflection lattice plane. The reflection occurs symmetrically as for the normal of the lattice plane but asymmetrically as for the surface.

Fig.11 shows typical throughput spectra from an undulator beamline at SPring-8. The broken curve shows a spectrum of the fundamental order light obtained for a fixed gap, and the solid curve, that obtained by synchronous tuning[24]. Photon number obtained at the sample position is 4×10^{12} $\cdot s^{-1}$ with $\Delta E/E = 2\times10^{-4}$ around 10 keV at 100 mA of stored current, and the beam size at the sample position is 1.5

mm (w)×0.6 mm (h) without using refocusing mirrors.

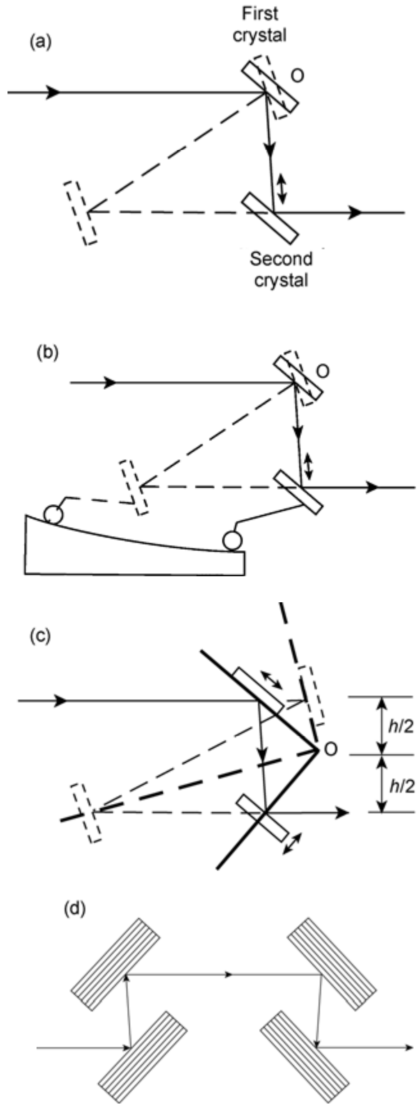

Fig.10 Schematics of crystal monochromators. (a), (b) and (c) double crystal monochromators, (d) 4-crystal monochromator. See detailed explanation in text.

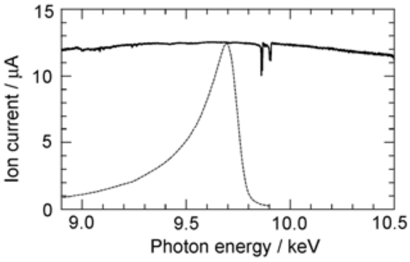

Fig.11 Throughput spectra from a double crystal monochromator (SPring-8)[24]. A plane undulator was used.

2.5 Filters

Generally the light from monochromators includes higher order light and scattered light caused by the dispersive elements, other than the monochromatic light. Therefore, such undesirable light has to be reduced. One way is to use reflection filter as mentioned in section 2.3.1. The other way is to use transmission filter. Above 105 nm, LiF, and other ionic crystals can be used as cutoff filters. In the 100-80 nm and 70-50 nm regions, self-standing films of In and Sn are used as band filters, respectively. In the shorter wavelength region, the core absorption feature, in which the absorption is much smaller below the core absorption edge than above the edge, is utilized. This feature can be seen in Fig.12. When one uses the light of energy E_1, purer dispersed light can be obtained by the use of the film which absorbs the light of energy E_2=2E_1. Furthermore, the film can be used as a band filter for a certain photon energy region below the core absorption edge to suppress the scattered light. Such absorption edges are located around 70 eV (Al *L*), 1.5 keV (Al *K*), 5 keV (Ti *K*), 8.3 keV (Ni *K*), 8.9 keV (Cu *K*), and so on.

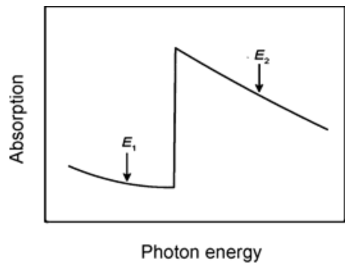

Fig.12 Schematic of absorption spectrum of a transmission filter.

3 Design consideration

3.1 Design consideration

What is the purpose of the experiment, and what characteristics of photon beam are required for the experiment, are essential to design the beamline, though a few or several kinds of experiments are often made at the same beamline. The required characteristics of the photon beam at the sample positions are photon energy, resolution, beam size and divergence, photon number, polarization characteristics, and so on. Important is how to construct a beamline which meets the requirements of the experiment. From the requirements, a type of monochromator is selected and conceptual design is made by the use of geometrical optics with choosing the kind of source, that is, light from a bending magnet or an undulator. To make the conceptual design, the following principle has to be kept in mind. The product of the size and the divergence of the light beam at the source point is conserved at any focusing point in the ideal optical system, which is called Lagrange invariant. This value is larger than the emittance of the electron beam. The photons are emitted in the invariant. The product of the size and the divergence of the light at the sample position is called acceptance of light at the sample. When the acceptance is smaller than the invariant, the available photon number is the flux given in section 1 reduced by the ratio of the acceptance to the invariant. Therefore, when a beam of large photon number in a small acceptance is required, the light from an undulator has to be used. When the acceptance is larger than the invariant, the available photon number is given by the flux. When a beam of large photon number is required in a somewhat large area, the light from a bending magnet or a multipole wiggler is also useful. When an intense light is required, unless its band width is required to be very small, the light from an undulator can be used without a monochromator, but with appropriate filters. In the conceptual design, requirements to pre-mirrors such as position, type, coating, angle of incidence, divergence angle of synchrotron radiation to be collected, size, those to dispersive elements such as position, type, groove spacing and shape, size, and those to refocusing mirrors, are decided on trial. As the aberration effect is not taken into account in the trial optical system, the configuration of the optical components has to be checked by the ray tracing. Through the checking procedure, conditions or configurations of optical system for better focuses on the entrance and the exit slits, and the sample position will be found. These procedures have to be made iteratively. Furthermore at the same time, the machinery, cooling, control, and vacuum systems of the beamline have to be designed conceptually from the stand point of view of actualization. These procedures are also iterative. Finally, whole requirements from instrumentation are taken into account and are made compatible, and the best and optimized system is designed. The qualities of optical elements, such as allowance of slope error and surface roughness, are specified.

3.2 Principle of ray tracing

Let the light coming from A (x,y,z) be reflected at P (w, l, h) on a mirror surface, and reach the position B (x',y',z') as shown in Fig. 13. The path from A to B is determined by Fermat's principle such that the path function defined as $F=AP+BP$ is minimized. When the reflector is a crystal, the situation is the same. However, in the case of a grating, a term $Nm\lambda$ should be added to the path function to satisfy the diffraction condition, where m is an integer representing the order of diffraction, and N is the number of grooves between the grating center O and the point P. The reason is as follows. The difference between path length of rays diffracted by different grooves should be a multiple of wavelength λ. Therefore the path function is given by $F=AP+BP+Nm\lambda$. In general, the number of grooves is given as

$$N=\frac{w}{d_0}+a_{20}w^2+a_{30}w^3+\cdots\cdots+a_{02}l^2+\cdots\cdots+a_{12}wl^2+\cdots\cdots \tag{5}$$

where d_0 is nominal groove space at the grating center ($w=l=0$). When $a_{20}=a_{30}=\cdots\cdots=a_{02}=\cdots\cdots=a_{12}=\cdots\cdots=0$, the groove space is constant. AP and BP are given as

$$AP=\sqrt{(x-w)^2+(y-l)^2+(z-h)^2} \tag{6}$$

$$BP=\sqrt{(x'-w)^2+(y'-l)^2+(z'-h)^2} \tag{7}$$

The surface of the reflector is expressed as $h=f(w,l)$. Therefore Fermat's principle is written as $\delta F/\partial w=\delta F/\partial l=0$. The relation between the directions of the incident and reflected (diffracted) light at the point P on the reflector (grating) is derived from Eqs. (6) and (7) as

$$\cos\xi'=-\cos\xi-(\cos\zeta+\cos\zeta')\frac{\partial h}{\partial w}+m\lambda\frac{\partial N}{\partial w} \tag{8}$$

$$\cos\eta'=-\cos\eta-(\cos\zeta+\cos\zeta')\frac{\partial h}{\partial l}+m\lambda\frac{\partial N}{\partial l} \tag{9}$$

$$\cos^2\xi'+\cos^2\eta'+\cos^2\zeta'=1 \tag{10}$$

where $\cos\xi$, $\cos\eta$, and $\cos\zeta$ are direction cosines of the incident light, and $\cos\xi'$, $\cos\eta'$, and $\cos\zeta'$, those of reflected light.

The electron beam on the orbit, to a certain extent having a cross section described in section 1, is the light source. It is divided into many portions and each portion is represented by one point. The light emitted from each point is simulated by many rays, with the divergent angles also described in section 1. They are distributed in an angle of acceptance of the optical system. The incident beam is represented by the light from such many *A* points with many divergence angles. The directions of the reflected (diffracted) rays can be calculated using Eqs. (8-10), and one can get the spot diagram consisting of many *B* points simulating the beam at any point of the optical path. For grating monochromators, one can design groove spacing to minimize the aberration. The programs of the ray tracing are available, for instance SHADOW[25].

Fig. 14 shows an example of the ray tracing results, the result of beamline BL8B1 at UVSOR[13]. The monochromator is of constant-arm type with gratings of constant groove spaces (see Fig. 8 (b)). The spot diagrams at the entrance slit and the sample position are shown in the figure. The cross section of the source was $2\sigma_x \times 2\sigma_y = 0.76\ \text{mm} \times 0.54\ \text{mm}$, and the angle of acceptance, 1.5 mrad (ver.) × 10 mrad (hor.). The spot diagram at the sample is that of the light passing through the entrance slit of 100 μm.

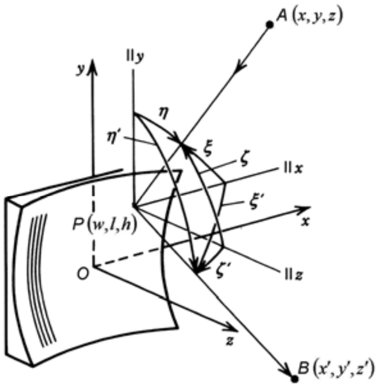

Fig.13 Coordinate in ray tracing.

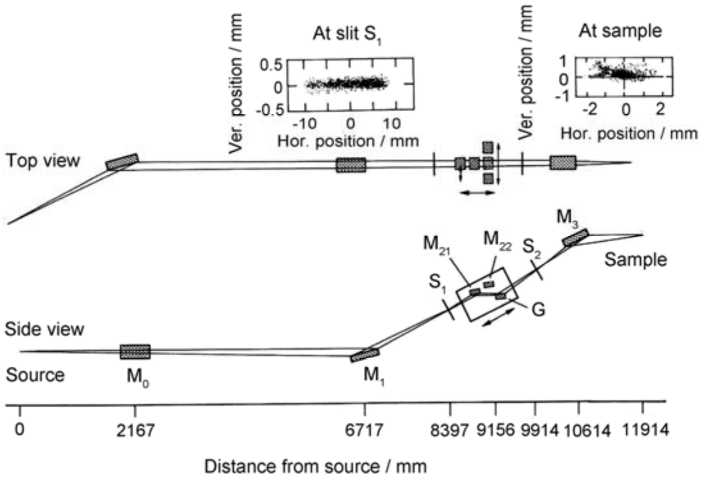

Fig.14 Optics of constant-arm monochromator[13].

3.3 Optical machinery and control

The mirrors with small radii can be made by polishing fused quartz, SiC, metals, and other materials, whereas the mirrors with large radii by bending some flexible plane mirrors. Crystals are also often bent. An example of sagittal bender of a second crystal of a DXM is shown in Fig. 15[26].

The heat load of the optical elements is a serious problem and cooling is very important. The power is given by the formula described in section 1. In some cases, the heat load exceeds a few $W\cdot mm^{-2}$ at the surface of the optical elements. They are usually indirectly cooled in such a way that they touch Cu plate, and the Cu plate is cooled directly. The water is used as coolant. Sometimes the crystals are directly cooled in such a way that the path of the coolant flow is made by directly cutting them as pin-posts or channels as shown in Fig. 16[27], and the crystals touch the coolant directly. Sometimes coolant is liquid N_2. Usually 3-dimensional finite element method is applied to simulate the deformation of optical elements irradiated by synchrotron radiation under the cooling.

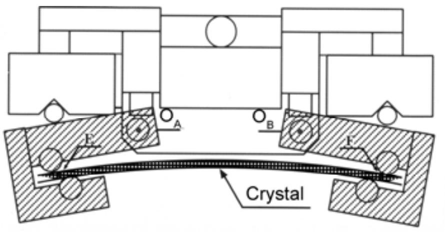

Fig.15 A sagittal-focusing crystal-bender[26].

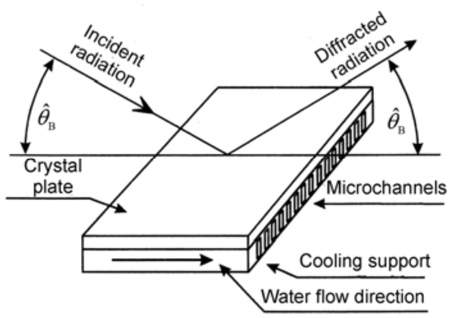

Fig.16 A cooling scheme of dispersive crystal[27].

The mirrors have to be set stable and furthermore, the fine adjustment of incident angles has to be made easily. Fig. 17 shows an example of mirror holders, where the mirror-chamber itself is adjusted[28]. The dispersive elements are rotated for wavelength scanning. In the case of VUV, it needs the rotation feedthrough of ultrahigh vacuum. In many cases, more than two dispersive elements are used with interchanging each other as seen in Fig. 14. This needs precise linear motion feedthrough of ultrahigh vacuum. Under this condition, the rotation angles have to be set with a precise mechanism from outside of the chamber.

The other important parts of monochromators are slits. The accuracy required to the slit width is of 1 μm order. The adjustment of the slit width from the outside of the chamber has to be guaranteed in ultrahigh vacuum, and under the high heat load of synchrotron radiation (sometimes the slits have to be cooled).

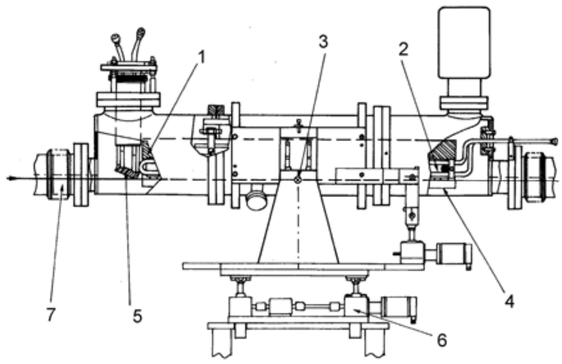

Fig.17 Chamber of pre-mirror (HASYLAB)[28].

1. Mirror, 2. Cooling plate, 3 Rotation axis, 4. Shield against Compton scattering, 5. Heat absorber, 6. Vertical adjuster, 7. Bellows.

A personal computer commands the selection of dispersive elements and their rotation. The position and the rotation angle have to be monitored by linear and rotational encorders, respectively. Such monitored signals are sent to the computer to make sure the movement. A movement smaller than 1 μm is available by the use of piezoelectric element. In this case, the real movement has to be also checked.

3.4 Vacuum

The VUV beamlines are connected to the light source directly, so that they have to satisfy the ultrahigh vacuum condition. This condition has an advantage to suppress the carbon contamination of optical element surfaces caused by photochemical reaction of synchrotron radiation, and residual hydrocarbon molecules, deteriorating reflectivity. The schematic of the vacuum chamber connected with a pump through an evacuating pipe is shown in Fig. 18. In the chamber, optical and other devices are omitted. The pressure p of the chamber is required to be ~10^{-8} Pa. The pressure is given as $p = Q/S_{\mathrm{eff}}$. Total outgas is given as $Q = Q_{\mathrm{T}} + Q_{\mathrm{SR}}$ (unit : Pa・L・s^{-1}), which is the summation of thermal desorption (Q_{T}), and desorption because of the irradiation of synchrotron radiation (Q_{SR}). $Q_{\mathrm{T}} = \sum_i s_i q_i$, where s_i and q_i are the surface area and the thermal outgassing rate of ith material, respectively. Usually Q_{SR} is larger than Q_{T}. S_{eff} stands for effective pumping speed which is given as $1/S_{\mathrm{eff}}=1/S+1/C$, where S is the pumping speed of the pump (unit : L・s^{-1}) and C, conductance of the evacuating pipe (unit : L・s^{-1}). When the pipe is cylindrical, the conductance is given as C=12.1 D^3/L (L・s^{-1}), where D is the diameter and L is the length of the pipe in cm. Therefore, the evacuating pipe has to be as wide and short as possible. It is of course important to clean the inner surface of the chamber and the surfaces of devices.

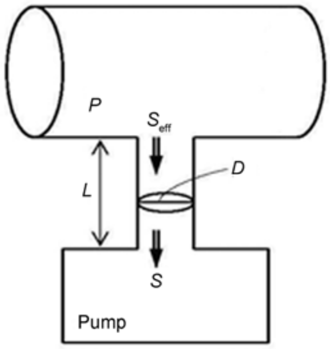

Fig.18 Pumping scheme of ultrahigh vacuum.

4 Polarization control

4.1 Polarizer

Many kinds of polarization studies have been made at synchrotron radiation beamline. They are polarization diagnosis of beamlines, polarimetry experiments, conversion of linearly polarized light to circularly polarized light, and others. For these studies polarizers are necessary. Here “polarizers” include analyzers and phase shifters. In usual VUV region, two kinds of polarizers are used. One is of multi-mirror type as shown in Fig.19 (a)[29]. It utilizes the difference in reflectivity. That is, the reflectivity of the perpendicular component of the light, of which electric vector is perpendicular to the plane of incidence, is larger than that of the parallel component. The reflection of 3 or 4 times enhances the difference. In short wavelength region, refractive indices are nearly equal to 1, so that the reflectivity of the perpendicular component is much larger than that of the parallel component, when angle of incidence is about 45° (quasi-Brewster angle). Multilayer polarizers are used utilizing this feature in VUV region, and crystal polarizers are used instead of multilayers in X-ray region (see Fig. 19 (b)). When the polarization measurements are carried out, multi-mirror reflectors, multilayers or crystals are rotated around the optical axis of the incident light. The multilayers and crystals can be also used in the transmission mode. The transmission type has the advantage of being used as phase shifter without changing the optical path[30,31]. It utilizes the fact that the phase difference of the transmitted light between the parallel and the perpendicular components is large below and above the Bragg angle. That is, the small deviation of angle $\hat{\theta}$ from the Bragg angle with signs of + and − around 45° gives positive or negative phase difference. Therefore, one can make a quarter-wavelength plate by making the phase shift ±90° with choosing appropriate deviation angle. In this case, the thickness is chosen, as the parallel component of the transmitted light is as strong as the perpendicular component. Some multi-mirror reflector also can be used as a phase shifter[29].

4.2 Polarization diagnosis of beamline

Even though synchrotron radiation has excellent polarization characters, the good performance of the beamline is inevitable to utilize them. Before carrying out polarimetry experiments, polarization diagnosis is required to check the performance. Here an investigation of polarization of beamline BL8B1 at UVSOR is introduced[31]. The multilayer of Al/YB_6 was used to analyze the polarization behind a monochromator. The multilayer was mounted on a rotating analyzer unit, which rotates as a whole with a detector around the axis of incident light. The angles of observation of synchrotron radiation were selected by an aperture situated in front of a pre-mirror. The output signals are shown in Fig. 20 (a). The abscissa means the rotation angle and the ordinate, the relative intensity. The angles of observation are −0.19 mrad (■) and 0.93 mrad (▲), where + means upside of median plane and −, downside. When the angle of observation is small, the amplitude of the sinusoidal curve is large, and when the angle is large, the amplitude, small. It means that the linear polarization becomes small and the light becomes elliptically polarized when the angle of observation is large. The ellipticity can be estimated. The result is compared with the theoretical value of linear polarization calculated against the angle of observation, as shown in Fig. 20 (b). The experimental values agree well with the theoretical ones. This means that the original polarization characters of synchrotron radiation predicted by theory are kept in BL8B1. Furthermore, it is concluded that the center of optical elements are set on the center of the light, and the polarization is good enough to carry out polarimetry experiments. The diagnoses of this kind have been made not only in VUV, but also in X-ray regions.

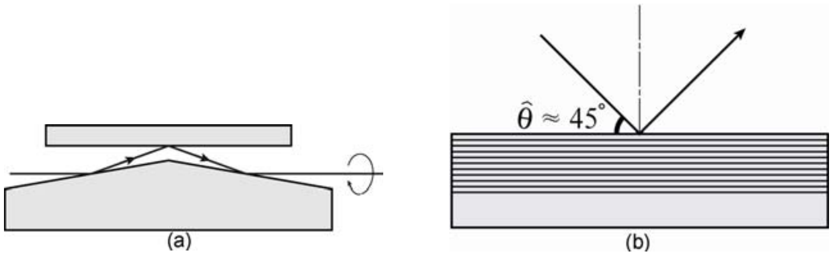

Fig.19 Polarizer. (a) 3-mirror reflector, (b) Multilayer/crystal.

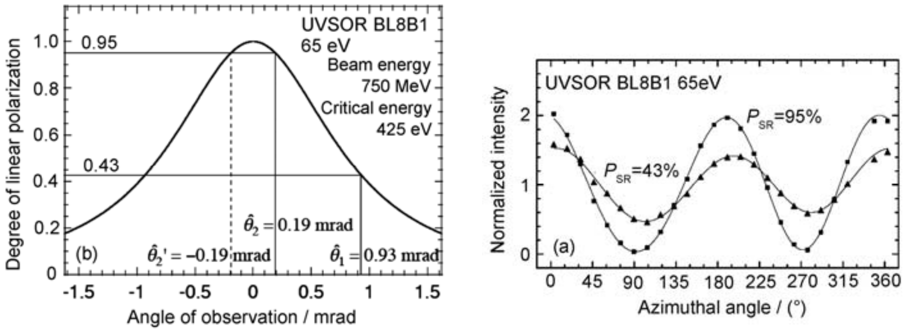

(a) (b)

Fig.20 Polarization diagnosis of BL8B1, UVSOR[31].

(a) Polarization signal (angle of observation, ■: − 0.19 mrad, ▲: 0.93 mrad),
(b) Experimental results of degree of linear polarization compared with the theoretical value of synchrotron radiation.

4.3 Circularly-polarized light generation

As an example of polarization control, the circularly-polarized light generation is introduced. Fig. 21 shows the schematic of this method[30]. The linearly-polarized light of synchrotron radiation of which electric vector is on the median plane (σ-polarized light), is dispersed by a DXM. In this configuration, the original linear-polarization character is kept at the exit slit. A polarizer made of a thin crystal acting as a quarter-wavelength plate is situated behind the DXM. The plane of incidence is not set on both horizontal and vertical planes, but on a plane rotated by 45° around the optical axis of the incident light from both planes. The reason why the plane of incidence is rotated by 45° is as follows. The electric vector of σ-polarized light consists of two components. One and another of them are on the planes rotated by 45° and −45°, respectively. Before the σ-polarized light enters the quarter-wavelength plate, the phases of both components are the same. When the light enters the plate and the angle of incidence deviates by even a small amount from Bragg angle, the phases of two components differ. When the deviation angle is chosen as the phase difference is ± 90°, the left and the right circularly-polarized light is obtained. Though the usable energy range is limited by the lattice constant of the crystal, this is a good way to generate the circularly-polarized light. Even though synchrotron radiation has a good circular polarization character, the dispersive crystals act as polarizers, so that the original source character is not necessarily kept behind the monochromators.

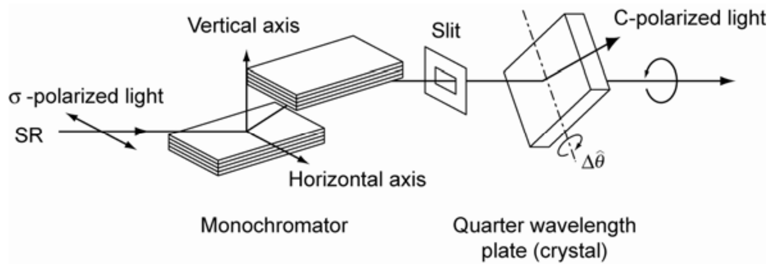

Fig.21 Scheme of circularly-polarized light generation from linearly-polarized light[30].

5 Summary

The beginnerusers and designers of the synchrotron radiation beamlines are asked to be versed in the basic concepts and technology of the beamlines, to carry out good experiments, and to design advanced and optimized beamlines, respectively. The basic concepts described here are the characteristics of synchrotron radiation, including the polarization characters and beamline technology to enable the experiments utilizing the characteristics. Further knowledge, such as detailed optics, monitors, detectors, stabilization of optical system, assembly of beamlines, computer control, and performance check, can be obtained from review articles[32-34]. When one intends to use a certain beamline, further knowledge to use it is needed, because each beamline has its own specification. Such specification can be obtained from a users' handbook at every facility. A person who is involved in designing a beamline needs further knowledge of optics and machinery of each beamline, which he/she considers. The discussion with future users is required. The progress in instrumentation of synchrotron radiation is very rapid, so that the designers need always to watch and gather new information. New information can be obtained from Proceedings of International Conference on Synchrotron Radiation Instrumentation, held every three years [35, 36].

References

1 Kunz C (ed). Synchrotron radiation: Techniques and applications. Berlin, Heiderberg (Germany): Springer-Verlag, 1979.

2 Winick H, Doniach S (eds). Synchrotron radiation research. New York (USA): Plenum Press, 1980.

3 Ma L, Yang F. (eds). Introduction to synchrotron radiation application. Shanghai (China): Fudan University Press, 2005 (in Chinese).

4 Watanabe M, Isoyama G. X-ray spectrometry: Recent technological advances, (ed. by Tsuji K, Injuk J, Van Grieken R), Chichester (UK): John Wiley & Sons, 2004:29.

5 Tanaka R, Kitamura H. SPECTRA, http://radiant.harima.riken.go.jp/spectra/index.html.

6 Watanabe M, Isoyama G. Dynamics during spectroscopic transition, (ed. by Lippert E, Macomber J D), Berlin, Heiderberg (Germany): Springer-Verlag, 1995:506

7 Suzuki S. unpublished.

8 Henke B L, Gullikson E M, Davis J C. At Data and Nucl Data Tables, 1993, **54**:181. See also http://www-crxo.lbl.gov/optical_constants/.

9 Yanagihara M, Yamashita K. X-ray spectrometry: Recent technological advances, (ed. by Tsuji K, Injuk J, Van Grieken R). Chichester (UK): John Wiley & Sons, 2004: 63.

10 Hatano T. Private communication.

11 Chen C T, Sette F, Rev Sci Instr, 1989, **60**:1616.

12 Senf F, Eggenstein F, Peatman W. Rev Sci Instr, 1992, **63**:1326.

13 Hiraya A, Nakamura E, Hasumoto M *et al*. Rev Sci Instr, 1995, **60**:2105.

14 Petersen H, Jung C, Hellwig C *et al*. Rev Sci Instr, 1995, **66**:1.

15 Hettrick M C, Underwood J H, Batson P J *et al*. Appl Opt, 1988, **27**:200.

16 Itou M, Harada T, Kita T. Appl Opt 1989, **28**:146..

17 Koike M, Namioka T. Rev Sci Instr, 1995, **66**:2144.

18 Tamenori Y, Ohashi H, Ishiguro E *et al*. Rev Sci Instr, 2002, **73**:1588.

19 Baron. Research frontier 2000/2001, SPring-8. Nishiharima (Japan): SPring-8, 2001.

20 Lemonnier M, Collet O, Depautex C, *et al*. Nucl Instr Meth, 1978, **152**: 109.

21 Matsushita T, Ishikawa T, Oyanagi H. Nucl Instr Meth, 1986, A**246**:377.

22 Murata T, Matsukawa T, Mori M *et al*. J de Phys, 1986, **47** C8:135.

23 Zhong Z, Kao C C, Siddons D P *et al*. J Appl Cryst, 2001, **34**:504.

24 Suzuki M. unpublished.

25 SHADOW, http://www.esrf.fr/computing/scientific/xop/shadowvui/.

26 Yoneda Y, Research frontier 1999/2000. Nishiharima (Japan): SPring-8, 2000:72.

27 Artemev A, Artemev N, Busetto E *et al*. Nucl Instr Meth, 2001, A**467**-**468**:380.

28 Hahn U, Gürtler P. Rev Sci Instr, 1995, **66**:2099.

29 Koide T, Shidara T, Yuri M, *et al*. Rev Sci Instr, 1992, **63**:1458.

30 Hirano K, Izumi K, Ishikawa T, *et al*. Jpn J Appl Phys, 1991, **30**:L407.

31 Hatano T, Hu W, Yamamoto M, *et al*. J Electr Spectr Rel Phenom, 1998, **92**:311.

32 Thompson A C, Vaughan D (eds). X-ray data booklet (LBNL/PUB-490R Rev.2). Berkeley (USA): Center for X-Ray Optics and Advanced Light Source, 2001.

33 Koch K K (ed.), Series of handbook on synchrotron radiation. North-Holland, 1983-1991.

34 Bilderback D H, Hodgson K O, Kiskinova M P, *et al*. Series on synchrotron radiation techniques and applications. Singapore: World Scientific, 1998.

35 Nucl Instr Meth, 2001, A**467**-**468.**

36 AIP Conf Proc (American Institute of Physics), 2004, **705**.